SIMULATION OF THE EFFECT OF FAR FIELD TSUNAMI THROUGH AN OPEN BOUNDARY CONDITION IN A BOUNDARY-FITTED CURVILINEAR GRID SYSTEM

Mohammed Ashaque Meah[1] , Ahmad Izani M Ismail[2], Md. Fazlul Karim[3], Md. Shafiqul Islam[1]

[1]*Department of Mathematics, Shahjalal University of Science & Technology, Bangladesh*
[2] *School of Mathematical Sciences, University Sains Malaysia, 11800 Pulau Pinang, Malaysia*
[3] *Faculty of Engineering, Institute Technology Brunei, Brunei*
Corresponding Author: Dr. Mohammed Ashaque Meah, Associate Professor, Dept of Mathematics, Shahjalal University of Science & Technology, Sylhet, Bangladesh. Phone: 88-0821-717850-256.
mamsust@yahoo.com ; izani@cs.usm.my; karimfazlul67@gmail.com ; msim5588@gmail.com

ABSTRACT

A new approach is developed to simulate the effect of far field tsunami in a limited area model domain where the coastal and Island boundaries are curvilinear in nature and the bending is high. The model is designed in a boundary fitted curvilinear grid system. To simulate the effect of far field tsunami, it is considered that the tsunami source is located far away from the model domain. The coastal and island boundaries and the other open boundaries of the model domain are represented by some functions so as to generate the boundary fitted grids. To use the regular finite difference scheme a transformation is used so that the physical domain is transformed into a rectangular one. The transformed shallow water equations are then solved in the transformed domain. The response of the tsunami source due to 26 December 2004 Indonesian tsunami is computed along the western open boundary of the model domain. Based on the response of the tsunami source, an appropriate boundary condition is formulated to simulate the effect of far field tsunami along the coastal belt. All simulations show excellent agreement with the observed data.

Key Words: *Boundary-fitted curvilinear grids*, *Open boundary condition, Far field tsunami, Shallow water equations, Tsunami source, Indonesian tsunami 2004.*

1. INTRODUCTION

The mega earthquake of 26 December 2004 with magnitude 9.3 occurred off the west coast of northern Sumatra of Indonesia and triggered a devastating tsunami. The tsunami waves spread across the Indian Ocean impacting and causing damage to the shores of more than a dozen countries throughout south and south east Asia. The catastrophic tsunami causes devastating damage not only on shores of neighboring countries but also on shores of more distant countries. It was clearly recorded by a large number of tide gauges throughout the world ocean, including tide gauges located in the North Pacific and North Atlantic (Rabinovich et al., 2006).

Tsunamis are called local, regional and far field or distant if the distances of the source are within 100 km, 100 – 700 km, and more than 700 km respectively from the coast. The three phases of a tsunami: generation, propagation and run-up are equally important for the accurate simulation of water levels in the coastal area for a near field or a local tsunami. But for distant tsunami the propagation phase becomes more important, since the time required for propagation is much longer than those for other phases (Yoon, 2002). However, the effect of a tsunami source along a particular coastal area far away from the region of interest may be significant if the waves move through deep Ocean. Since the response of the 2004 Indonesian tsunami reached every distant corner of the globe, it is necessary to estimate the response along a particular region due to a source located far away from that region. This may be done through a global model that contains both the source and the region of interest.

Kowalik et al. (2005) developed a global model to simulate the tsunami wave characteristics along the coastal belts throughout the globe associated with 2004 Indonesian tsunami. Arcas and Titov (2006) computed a worldwide tsunami propagation simulation of Sumatran tsunami of 2004 to compare their computational results with the stream of tide gage data from around the globe. However a global model is very expensive in terms of both computer storage and CPU time and is not suitable for real time simulation. In hydrodynamical computations problem arises when the theoretical model applies to an infinite or semi-infinite region. In this case, where the original domain of the problem under investigation is infinite or very large, open boundaries may be used. An open boundary is an artificial boundary of a computational domain through which propagation of waves or flow should pass in order to leave the computational domain without giving rise to spurious reflection (Joolen et. al. 2003). The main purpose of using the open boundaries is to enable waves and disturbances which originate from within the model domain to leave the model domain without affecting the interior solution of the mathematical model.

According to Yoon (2002), the prevention and mitigation of tsunami hazards depend on the accurate assessment of the generation, propagation and run-up of tsunamis. So, efforts should be made to construct mathematical (numerical) models. In particular regional tsunami numerical models should be developed to develop the early warning system. A number of studies have been done on modeling the Indonesian tsunami of 2004 for the west coast of Southern Thailand and Peninsular Malaysia after the event 26 December 2004 (Roy and Ismail, 2005; Roy et al., 2006; Karim et al., 2006). A lot of other researchers (e.g. Agarwal et al., 2005; Cho et al., 2007; Zahibo et al., 2006) have also modeled the 2004 Indian Ocean event. Then majority of the studies are based on depth-averaged shallow water equations and were discretized by the finite-difference Cartesian grids with the coastline represented by stair-steps. With a stair-step model the coastal boundaries are approximated

along the nearest finite difference gridlines of the numerical scheme (Roy, 1999). Though the finite difference grids with the coastline represented by stair-steps technique is often used in traditional hydrodynamic models of coastal currents like a tsunami, the computational costs have become excessive and affects the model accuracy negatively. To resolve the lateral geometry better, refined lateral grids should be used in finite difference models by using a large number of grids within the model domain (Bao et al., 2000). Since the accuracy of a stair step model depends on the grid size the grid spacing should be made small enough. So the computational coasts often become excessive.

On the other hand boundary-fitted curvilinear grid systems combines the best aspects of finite-difference discretization with grid flexibility. The boundary fitted grid technique makes the equations and boundary conditions simple and better represents the complex geometry with relatively less grid points. Thus, it significantly improves the finite difference schemes (Bao et al. 2000). The use of this kind of grid system allows the user extensive control over the design of the computational mesh. However one difficulty in boundary fitted grid system is that the gridline of the numerical scheme are curvilinear and non-orthogonal. In order to apply a regular finite difference scheme the grid system must be rectangular. In a boundary-fitted model, the curvilinear boundaries are transformed into straight ones using appropriate transformations, so that in the transformed space regular finite difference techniques can be used.

Karim et al. (2007) developed a shallow water model using a boundary fitted curvilinear grid system to simulate the 2004 Indonesian tsunami along the coastal belts of Phuket and Penang. Roy et al. (2006) presented a technique to compute the effect of a far field tsunami along the coastal belts by formulating an open boundary condition where the tsunami source is removed during the far field tsunami computation. The main goal of this study is to simulate the effect of a far field tsunami along the coastal belt of Phuket and Penang Island through an open boundary condition in a boundary fitted curvilinear grid system. For this purpose the boundary fitted curvilinear grid model of Karim et al. (2007) is used as the source model to compute the response of the source of Indonesian tsunami 2004 along the western open boundary of the model. Using the technique of Roy et al. (2006) and based on the data computed from the source model, an appropriate boundary condition is formulated along the western open boundary of the boundary fitted curvilinear grid model and at the same time the tsunami source near Sumatra is removed. This boundary condition is applied in the absence of the source in the model domain to simulate the effect of far field tsunami. Thus for far field tsunami computation instead of considering a tsunami source inside the model domain, an open boundary condition is imposed as an effect of a tsunami source.

2. GOVERNING EQUATIONS AND BOUNDARY CONDITIONS

The shallow water equations, which describe the inviscid flow of a shallow fluid in two dimensions, have been used for many years testing numerical methods for solving atmospheric and oceanic problems (Haltiner and Williams, 1980). These are coupled first order non-linear hyperbolic partial differential equations and are often used governing equations approximating tsunami propagation in the deep ocean as well as in near-shore regions including inundation (Aizinger and Dawson, 2002).

The displaced position of the free sea surface from the mean sea level is considered as $z = \zeta(x, y, t)$ and the sea floor as $z = -h(x, y)$ so that, the total depth of the fluid layer is $\zeta + h$.

Following Roy (1998), the vertically integrated shallow water equations for tsunami computations are

$$\frac{\partial \zeta}{\partial t} + \frac{\partial}{\partial x}\left[(\zeta + h)u\right] + \frac{\partial}{\partial y}\left[(\zeta + h)v\right] = 0 \tag{1}$$

$$\frac{\partial u}{\partial t} + u\frac{\partial u}{\partial x} + v\frac{\partial u}{\partial y} - f v = -g\frac{\partial \zeta}{\partial x} - \frac{C_f u(u^2 + v^2)^{1/2}}{\zeta + h} \tag{2}$$

$$\frac{\partial v}{\partial t} + u\frac{\partial v}{\partial x} + v\frac{\partial v}{\partial y} + f u = -g\frac{\partial \zeta}{\partial y} - \frac{C_f v(u^2 + v^2)^{1/2}}{\zeta + h} \tag{3}$$

where u and v are the velocity components of flow particle in x and y directions, f is the Coriolis parameter, g is the acceleration due to gravity, C_f is the friction coefficient.

For numerical treatment it is convenient to express the equations (2) & (3) in the flux form by using the equation (1). The shallow water equations in flux forms are

$$\frac{\partial \zeta}{\partial t} + \frac{\partial \tilde{u}}{\partial x} + \frac{\partial \tilde{v}}{\partial y} = 0 \tag{4}$$

$$\frac{\partial \tilde{u}}{\partial t} + \frac{\partial (u\tilde{u})}{\partial x} + \frac{\partial (v\tilde{u})}{\partial y} - f\tilde{v} = -g(\zeta + h)\frac{\partial \zeta}{\partial x} - \frac{C_f \tilde{u}\left(u^2 + v^2\right)^{1/2}}{\zeta + h} \tag{5}$$

$$\frac{\partial \tilde{v}}{\partial t} + \frac{\partial (u\tilde{v})}{\partial x} + \frac{\partial (v\tilde{v})}{\partial y} + f\tilde{u} = -g(\zeta + h)\frac{\partial \zeta}{\partial y} - \frac{C_f \tilde{v}\left(u^2 + v^2\right)^{1/2}}{\zeta + h} \tag{6}$$

where, $(\tilde{u}, \tilde{v}) = (\zeta + h)(u, v)$

Here u and v in the bottom stress terms of (2) and (3) have been replaced by $\tilde{u}$ and $\tilde{v}$ in (5) and (6) in order to solve the equations in a semi-implicit manner. $\tilde{u}$ and $\tilde{v}$ are the depth-averaged volume fluxes in the x and y directions, respectively.

According to Tang and Grimshaw (1996), open boundary conditions arise in numerical simulation of coastal ocean model and they play a role in determining the validity of the result. Numerical open boundary conditions should allow fluid motions generated in the computational domain and which are left at the open boundary to pass through the boundary without influencing the interior solution. They are imposed along the edge of the model domain where the solution is unknown. Open boundaries contrast to other boundaries where the solution can be specified from data, models, or assumed. Since the solution is unknown along the open boundaries an assumption must be made or the interior solution extrapolated (Roed and Cooper, 1986). For convenience of the treatment of boundary conditions, open boundaries are usually placed along coordinate axes.

The appropriate boundary condition along the coastal boundary is that the normal component of the vertically integrated velocity vanishes at the coast and following Roy (1998) this may be expressed as:

$$u\cos\alpha + v\sin\alpha = 0 \qquad \text{for all } t \geq 0 \tag{7}$$

where α is the inclination of the outward directed normal to the x-axis. It then follows that $u = 0$ along y- boundaries and $v = 0$ along the x- boundaries.

At the open-sea boundaries the waves and disturbance, generated within the model domain, are allowed to leave the domain without affecting the interior solution. Thus the normal component of velocity cannot vanish and so a radiation type of boundary is generally used. Following Heaps (1973), the following radiation type of condition may be used:

$$u\cos\alpha + v\sin\alpha = -(g/h)^{1/2}\zeta \quad \text{for all } t \geq 0 \tag{8}$$

Note that the velocity structure in a shallow water wave is described by $w = \dfrac{g\zeta}{\sqrt{gh}}$, where w is the horizontal particle velocity.

3. GENERATION OF BOUNDARY-FITTED GRIDS

The *OX* points are considered towards the west and *OY* points towards the north. The eastern coastal boundary, along y-axis, is situated at $x = b_1(y)$ and the western open-sea boundary, parallel to y-axis, is at $x = b_2(y)$. The southern open-sea boundary, along x-axis, and the northern open-sea boundary, parallel to x-axis, are at $y = 0$ and $y = L$ respectively. This configuration is shown in Fig. 1.
Following Roy (1999), the system of gridlines oriented to $x = b_1(y)$ and $x = b_2(y)$ are given by the generalized function

$$x = \{(k-l)b_1(y) + lb_2(y)\}/k \tag{9}$$

where $k = M$, the number of gridlines in x-direction and l is an integer and $0 \leq l \leq k$.
The system of gridlines oriented to $y = 0$ and $y = L$ are given by the generalized function

$$y = \{(q-p)0 + pL\}/q \tag{10}$$

where $q = N$, the number of gridlines in y-direction and p is an integer and $0 \leq p \leq q$.
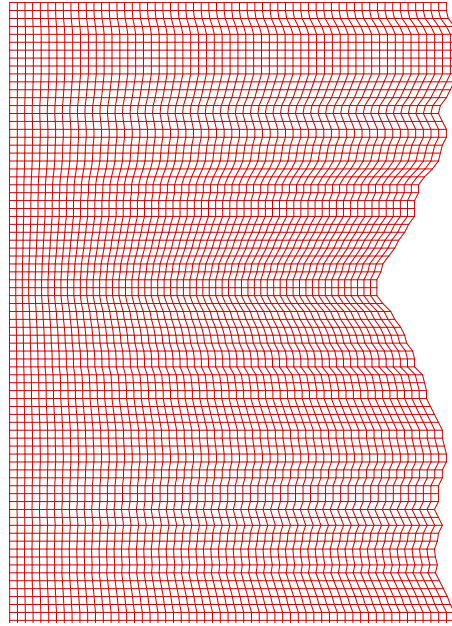
Figure 1. Boundary fitted grids in physical domain.
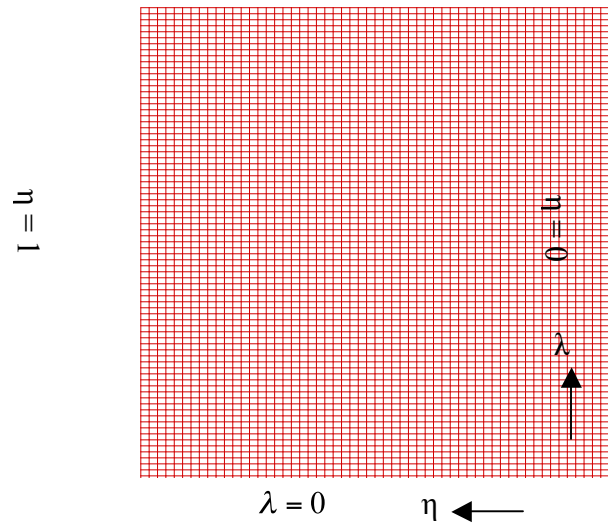
Figure 2. Transformed domain and the rectangular grid lines.

Note that equation (9) reduces to $x = b_1(y)$ and $x = b_2(y)$ for $l = 0$ and $l = k$ respectively. Similarly equation (10) reduces to $y = 0$ and $y = L$ for $p = 0$ and $p = q$ respectively. Now by proper choice of l, k and p, q the boundary-fitted curvilinear grids can be generated.

Every boundary of each island inside the model domain has been broken into several segments and every segment has been aligned either along (9) or along (10) so that the boundary of every island is aligned along the boundary fitted gridlines (Roy, 1999). The representation of the island boundaries are done this way so that the whereabouts of them have not been lost in the transformed domain. Each of the eastern and western boundaries of an island is given by (9) and each of the southern and northern boundaries of an island is given by (10).

Since $l = 0$ implies $x = b_1(y)$ or $\eta = 0$, the coastal boundary and $l = k$ implies $x = b_2(y)$ or $\eta = 1$, the open boundary, equation (9) with two different values of l, say, l_1 and l_2 with $l_1 < l_2$ will express the eastern and western boundaries of an island. Similarly equation (10) with two different values of p, say p_1 and p_2 with $p_1 < p_2$ will express the south and north boundaries of the island. Thus the transformed boundaries of an island are expressed as

$$\eta = l_1 / k, \ \eta = l_2 / k, \ \lambda = p_1 / q, \ \lambda = p_2 / q \tag{11}$$

For $x = b_1(y)$, the boundary condition (7) may be simplified as $u + v \tan \alpha = 0$, which gives $u - v\dfrac{dx}{dy} = 0$, that yields $u - v\dfrac{db_1}{dy} = 0$. Therefore, following Johns et al. (1981), the boundary conditions are given by

$$u - v\frac{db_1}{dy} = 0 \qquad \text{at } x = b_1(y), \text{ along } x\text{-axis} \tag{12}$$

$$u - v\frac{db_2}{dy} = (g/h)^{1/2}\zeta \qquad \text{at } x = b_2(y), \text{ parallel to } y\text{-axis} \tag{13}$$

$$v + (g/h)^{1/2}\zeta = 0 \qquad \text{at } y = 0, \text{ along } x\text{-axis} \tag{14}$$

$$v - (g/h)^{1/2}\zeta = 0 \qquad \text{at } y = L, \text{ parallel to } x\text{-axis} \tag{15}$$

4. COORDINATE TRANSFORMATION

To facilitate the numerical treatment of an irregular boundary configuration, a transformation of coordinates used is. The transformation is similar to that in Johns et al. (1985), which is based upon new set independent variables η, λ, y, t where

$$\eta = \frac{x - b_1(y)}{b(y)}, \quad \lambda = \frac{y}{L}, \quad b(y) = b_2(y) - b_1(y). \tag{16}$$

This mapping transforms the analysis area enclosed by $x = b_1(y), x = b_2(y), y = 0$ and $y = L$ into a rectangular domain given by $0 \le \eta \le 1, \ \ 0 \le \lambda \le 1$ (Fig. 2).

The generalized function (9) takes the form $b\eta + b_1 = \{(k-l)b_1(y) + lb_2(y)\}/k$, which can be written as $\eta = \dfrac{l(b_2 - b_1)}{bk}$ and this gives

$$\eta = \frac{l}{k}. \tag{17}$$

The generalized function (10) takes the form $\lambda L = \{(q-p)0 + pL\}/q$, which gives

$$\lambda = \frac{p}{q}. \tag{18}$$

For $l = 0$, we have the eastern coastal boundary $\eta = 0$ or $x = b_1(y)$ and for $l = k$, we have the western open-sea boundary $\eta = 1$ or $x = b_2(y)$. Similarly, for $p = 0$, we have the southern open sea boundary $\lambda = 0$ or $y = 0$ and for $p = q$ we have the northern open-sea boundary $\lambda = 1$ or $y = L$. Thus by the proper choice of the constants k and q and the parameters l and p, rectangular grid system can be generated in the transformed domain.

5. TRANSFORMED SHALLOW WATER EQUATIONS AND BOUNDARY CONDITIONS

By using the transformations (16),

$$\frac{\partial}{\partial x} \equiv \frac{1}{b}\frac{\partial}{\partial \eta} \tag{19}$$

$$\frac{\partial}{\partial y} \equiv -\frac{1}{b}\left(\frac{db_1}{dy} + \eta\frac{db}{dy}\right)\frac{\partial}{\partial \eta} + \frac{1}{L}\frac{\partial}{\partial \lambda} \tag{20}$$

Taking η, λ, y, t as the new independent variables and using the relations (19) and (20), the equations (4) – (6) transform to (by Karim et al., 2007)

$$\frac{\partial(bL\zeta)}{\partial t} + \frac{\partial \tilde{U}}{\partial \eta} + \frac{\partial \tilde{V}}{\partial \lambda} = 0 \tag{21}$$

$$\frac{\partial \tilde{u}}{\partial t} + \frac{\partial (U\tilde{u})}{\partial \eta} + \frac{\partial (V\tilde{u})}{\partial \lambda} - f\tilde{v} = -gL(\zeta + h)\frac{\partial \zeta}{\partial \eta} - \frac{C_f \tilde{u}\left(u^2 + v^2\right)^{1/2}}{\zeta + h} \tag{22}$$

$$\frac{\partial \tilde{v}}{\partial t} + \frac{\partial (U\tilde{v})}{\partial \eta} + \frac{\partial (V\tilde{v})}{\partial \lambda} + f\tilde{u} = -g(\zeta + h)\left[b\frac{\partial \zeta}{\partial \lambda} - L\left(\frac{db_1}{dy} + \eta\frac{db}{dy}\right)\frac{\partial \zeta}{\partial \eta}\right] \tag{23}$$

$$- \frac{C_f \tilde{v}\left(u^2 + v^2\right)^{1/2}}{\zeta + h}$$

where, $U = \dfrac{1}{b}\left[u - \left(\dfrac{db_1}{dy} + \eta\dfrac{db}{dy}\right)v\right]$, $V = \dfrac{v}{L}$, $(\tilde{u}, \tilde{v}, \tilde{U}, \tilde{V}) = bL(\zeta + h)(u, v, U, V)$

At $x = b_1(y)$ i.e. at $\eta = 0$, $U = \dfrac{1}{b}\left[u - \left(\dfrac{db_1}{dy} + \eta\dfrac{db}{dy}\right)v\right] = \dfrac{1}{b}\left[u - \dfrac{db_1}{dy}v\right] = 0$.

And at $x = b_2(y)$ i.e. at $\eta = 1$, $U = \dfrac{1}{b}\left[u - \left(\dfrac{db_1}{dy} + 1\cdot\dfrac{db}{dy}\right)v\right] = \dfrac{1}{b}\left[u - \dfrac{db_2}{dy}v\right]$, which gives

$bU = u - \dfrac{db_2}{dy}v$.

Therefore the boundary conditions (12) – (15) reduces to

$U = 0$	at $\eta = 0$	(24)
$bU - (g/h)^{1/2}\zeta = 0$	at $\eta = 1$	(25)
$VL + (g/h)^{1/2}\zeta = 0$	at $\lambda = 0$	(26)
$VL - (g/h)^{1/2}\zeta = 0$	at $\lambda = 1$	(27)

At each boundary of an island, the normal component of the velocity vanishes. Thus, the boundary conditions of an island are given by

U = 0	at $\eta = l_1/k$ and $\eta = l_2/k$	(28)
V = 0	at $\lambda = p_1/q$ and $\lambda = p_2/q$	(29)

6. GRID GENERATION IN TRANSFORMED DOMAIN WITH FINITE DIFFERENCE SCHEME

Since the analysis area or the physical domain is transformed into a rectangular one, the rectangular grid system is generated in the analysis area using a set of equidistant straight lines parallel to η-axis and a set of equidistant straight lines parallel to λ-axis. The space between any two consecutive gridlines parallel to λ-axis is $\Delta\eta$ and that between any two consecutive gridlines parallel to η-axis is $\Delta\lambda$. Let there be M gridlines parallel to λ-axis and N gridlines parallel to η-axis. So, there are M grid points in η-direction and N grid points in λ-direction and the total number of grid points is $M \times N$.

We define the grid points (η_i, λ_j) in the domain by

$\eta_i = (i-1)\Delta\eta,$	$i = 1, 2, 3, \ldots, M$	(30)
$\lambda_j = (j-1)\Delta\lambda,$	$j = 1, 2, 3, \ldots, N$	(31)

The sequence of discrete time instants is given by

$$t_k = k\,\Delta t, \qquad k = 1, 2, 3, \ldots \tag{32}$$

A staggered grid system, similar to Arakawa C system (Arakawa and Lamb, 1977), is used in the transformed domain where there are three distinct types of computational points. These three types of points are defined as follows: For every discrete grid point (η_i, λ_j), if i even and j odd, the point is a ζ-point at which ζ is computed. If i is odd and j is odd, the point is a u-point at which u is computed. If i is even and j is even, the point is a v-point at which v is computed. In a staggered grid system, since every dependent variable is computed at any one of these three types of points rather than at every point, the CPU time is reduced. Moreover, a staggered grid system is favorable in filtering out sub-grid scale oscillations.

The transformed shallow water equations (21) - (23) together with the boundary conditions (25) - (27) are discretized by finite difference (Forward Time Centered Space) and are solved by a conditionally stable semi-implicit method.

The η-axis is directed towards west at an angle 15° (anticlockwise) with the latitude line and the λ-axis is directed towards north inclined at an angle 15° (anticlockwise) with the longitude line. In this model the analysis area is extended from 2° N to 14° N latitudes (incorporating the west coasts of Malaysia including Penang and Southern Thailand including Phuket) and 91° E to 101.5° E longitudes (Fig. 3).
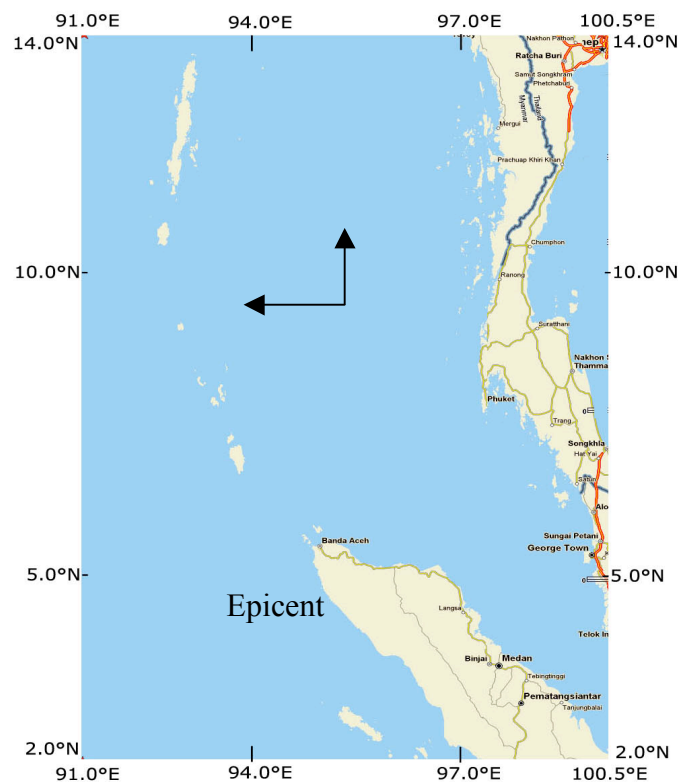
Figure 3. Model Domain including the coastal geometry and the epicenter of the 2004 earthquake (Courtesy: Roy et al., 2006).

The number of grids in η and λ - directions are respectively $M = 230$ and $N = 319$. The model area includes the source region of Indonesian tsunami 2004. On the ocean boundary, radiation condition, in which the tsunami wave is assumed to go out without changing its shape, is assumed. For the land boundary (i.e the coast), it is assumed there is total reflection. The coastal boundary is fixed; i.e. we assume no run-up on the land. The time step of computation is determined to satisfy the stability condition. It is set to 10 s in this computation. Following Kowalik et al. (2005), the value of the friction coefficient C_f is taken as 0.0033 through out the model area. The available depth data for some representative grid points of the model area are collected from the Admiralty bathymetric charts. The depth at the entire rest grid points of the mesh are computed by some averaging process. The bathymetry of the modal domain is shown in the Fig. 4.
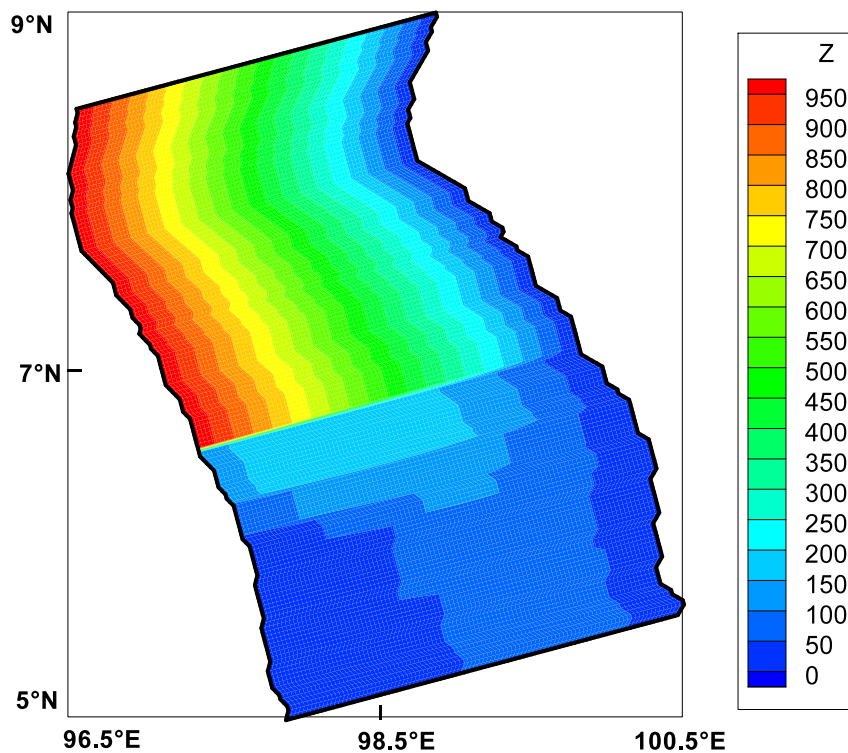
Figure 4. Bathymetry used in the numerical simulation (depth unit: m).

7. TSUNAMI SOURCE GENERATION AND INITIAL CONDITIONS

For tsunami computation initialization of model geometry, various parameters and variables is required first. The tsunami generation is modelled by the initialisation of the water surface. The generation of an earthquake tsunami source depends essentially on the pattern and dynamics of motions in the earthquake source zone and on the initial seafloor movements. The generation mechanism of the 2004 Indonesian tsunami was mainly a static sea floor uplift caused by an abrupt slip at the India/Burma plate interface. A detailed description of the estimation of the extent of the earthquake rupture as well

as the maximum uplift and subsidence of the seabed is given in Kowalik et al. (2005) and this estimation is based on seismological methods in Okada (1985). From the deformation contour, it was concluded that the estimated uplift and subsidence zone is between 92° E to 97°E and 2°N to 10°N with a maximum uplift of 507 cm at the west and maximum subsidence of 474 cm at the east. The uplift to subsidence is approximately from west to east relative to the west coasts of the Malaysian Peninsula and Thailand. The major force of tsunamis is the vertical displacement of the seafloor. For computational purposes tsunami models are often initialized by a sea-surface displacement. We can assume that the initial value of the sea surface displacement that starts a tsunami is the same as the vertical displacement of the sea floor (Arreaga-Vargas et al., 2005; Aida, 1974), due to incompressibility of the ocean water. The assumption is taken with an instantaneous source approximately with the length of the rupture zone (the area covered by the initial aftershock distribution). Following Kowalik et al. (2005) the disturbance in the form of rise and fall of sea surface is assigned as the initial condition in the source model with a maximum rise of 5 m to maximum fall of 4.75 m to generate the response of the tsunami along the western open boundary of the model domain. In all other regions of the domain the initial sea surface deviations are taken as zero. Also the initial x- and y-components of the velocity are taken as zero throughout the model area.

8. OPEN BOUNDARY CONDITION FOR FAR FIELD TSUNAMI COMPUTATION

The time series of the sea surface fluctuation and amplitude of the source of Indonesian tsunami 2004 along the western open boundary of the model has been computed. To simulate the far field tsunami or to investigate the effect of a far field tsunami it is considered that the tsunami source is located far away from the model domain. The amplitudes of tsunami wave along the western open boundary as the response of the source has been computed to estimate the amplitude of the boundary condition by which far field tsunami will be computed in absence of the source.

For generating tidal oscillation in a limited area model through a boundary, the open boundary condition is generally formulated by associating a sinusoidal term, containing amplitude, period and phase, with the radiation type of boundary condition (Johns et al., 1985; Roy, 1995) and this is described as

$$u - \sqrt{g/h}\, \zeta = -2\sqrt{g/h}\, a \sin\left(2\pi t/T + \varphi\right), \text{ at } x = b_2(y) \tag{33}$$

where a is the amplitude, T is the period, φ is the phase of the wave. But for tsunami propagation the time series is oscillatory with damping amplitude. On the basis of time series data and amplitude, the open boundary condition that represents the effect of far field tsunami for the boundary fitted curvilinear model is (Roy et al., 2006)

$$bU - \sqrt{g/h}\, \zeta = -2\sqrt{g/h}\, e^{(-st)} a \sin(2\pi t/T + \varphi), \text{ at } x = b_2(y) \tag{34}$$

where s is the scale factor used for damping the amplitude of the wave with respect to time. In equation (34), the following conditions are imposed:
$s = 0$ for $t \leq T$ and $s > 0$ for $t > T$.

Through this condition we are allowing one wave, with full amplitude, to enter into the domain through the open boundary before damping of the amplitude begins.

The assigned amplitudes (*a*) in (34) are adjusted so that the response of the boundary condition in model domain is similar to that associated with the source of Indonesian tsunami 2004. By trial and error method, the values of phase (*φ*), period (*T*) and the scale factor in equation (34) have also been adjusted and these are *φ* = 0, *T* = 0.5 hr and *s* = 0.01. Fig. 5 shows the time series of sea surface fluctuation at (230, 155) th grid point at the western open boundary due to the source of Indonesian tsunami 2004 and the boundary condition. Both the time series are found to be almost identical, which means that the boundary condition is capable of generating time series which is similar to that generated by the source.
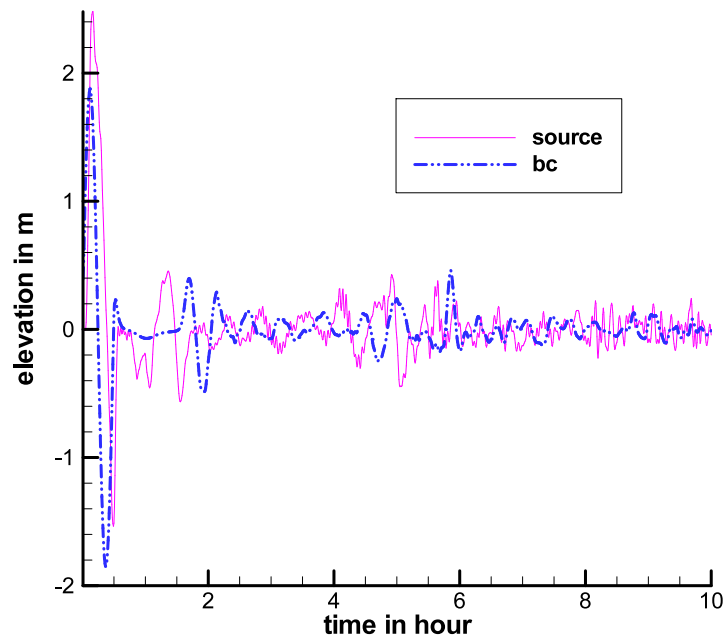
Figure 5. Time series of sea surface fluctuation at the western open boundary.

9. SIMULATION OF 2004 TSUNAMI THROUGH THE OPEN BOUNDARY CONDITION

In this section, the propagation of water waves generated by the open boundary condition without considering the tsunami source of 2004 Indian ocean earthquake inside the model domain is studied. Tsunami travel time towards the two coastal locations and the time series of water elevation due to the open boundary condition are also presented. Finally, the contour of the maximum water level at different coastal locations is also presented. The computed results are compared with those recorded and observed data.

The arriving time of tsunami at the coast has been studied. Fig. 6 shows the contour plot of time, in minutes, for attaining +0.1 m sea level rise at each grid point in the model domain. Thus considering the 0.1 m sea level rise as the arrival of tsunami, it is seen that after imposition of the boundary condition, the disturbance propagates gradually towards the coast. The arrival time of tsunami due to the boundary condition at Phuket is 150 min and the same at Penang is approximately 270 min. If the source is considered within the model domain, the arrival time of tsunami from the source at Phuket and Penang islands are 110 min and 240 min respectively (Karim et al., 2007). In the present study the response of the open boundary condition imposed at the west boundary has been computed, which is away from the source zone of the Indonesian tsunami 2004. This is why the computed arrival time is delayed by up to 30 to 40 min compared to the arrival time when the source is considered within the model domain. This time difference can be estimated by measuring the total distance of the open boundary from the coast and tsunami travel time due to the boundary condition. Thus the corrected time related to the tsunami source at Sumatra should be 30 to 40 min earlier than the present computed time. In the USGS website it is reported that the tsunami waves reached at Phuket within two hours time after the earthquake and the arrival time of tsunami at Penang is between 3 hr 30 min and 4 hours. Thus the tsunami travel time along the coastal and island boundaries of Phuket and Penang computed by the open boundary condition agree well with the data available in the USGS website.
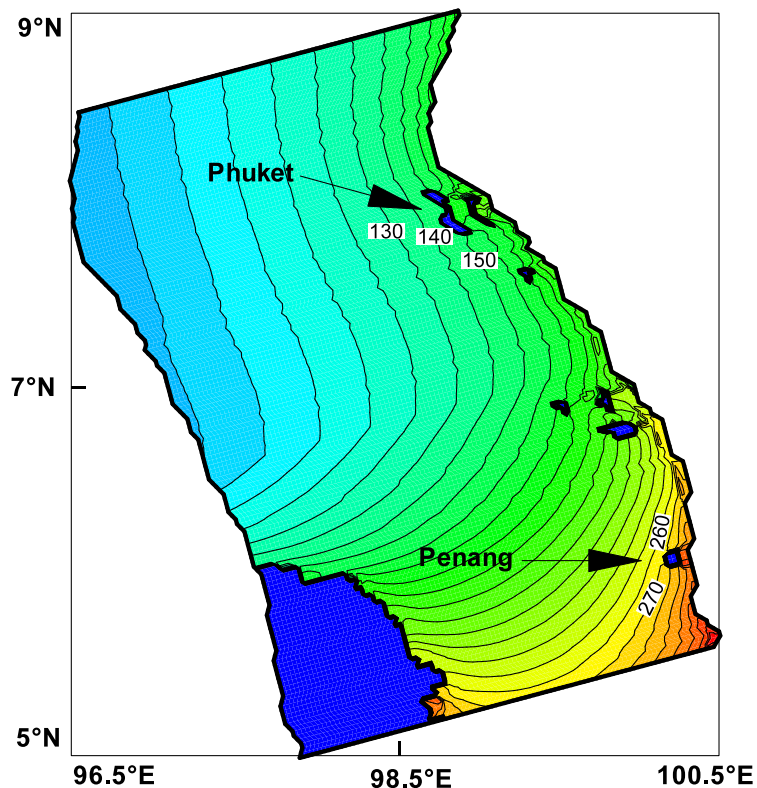

Figure 6. Tsunami propagation time in minutes towards Phuket and Penang due to the boundary condition.

Fig. 7 depicts the maximum water level contours, along the coast from Penang Island to Phuket. The surge amplitude is increasing from south to north; the maximum water level at Penang Island is from 2 m to 4 m, whereas the same at Phuket region is 6 m to 11 m. The computed water levels indicate that the north and west coasts of Penang Island and the north-west part of Phuket are at risk of highest surge due to the source at Sumatra. The maximum coastal surge estimated by the boundary condition varies from 18 - 20 m in some locations located approximately 50 km north from the Phuket. Tsuji et al. (2006) reported that the largest tsunami height reached up to 19.6 m at Ban Thung Dap located at 50 km north from the Phuket. Thus the model result shows a quite good agreement with the study of Tsuji et al. (2006) for the Phuket region.
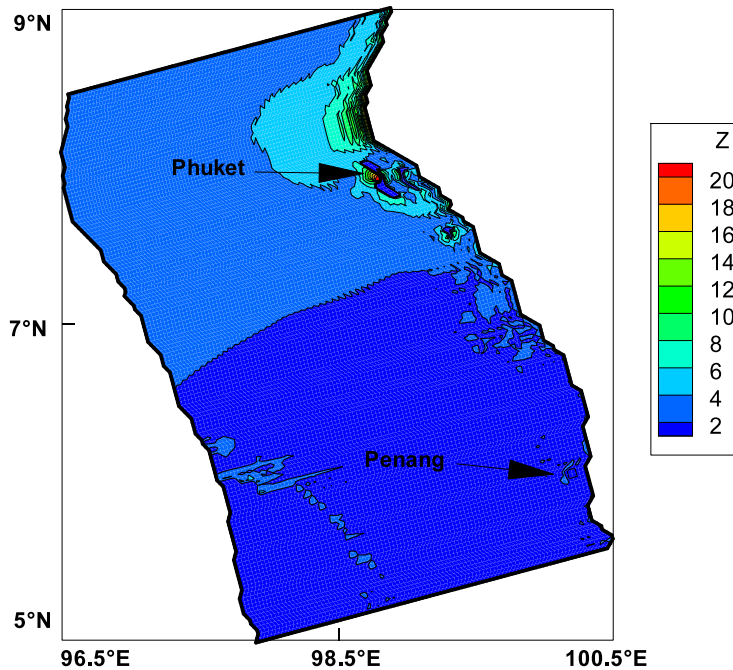

Figure 7. Contour of maximum water elevation due to the boundary condition around the west coast of Thailand and Malaysia.

The computed water levels at different locations of the coastal belt of Phuket and Penang Island are stored at an interval of 30 seconds. Fig. 8 depicts the time series of water levels for the Phuket region in south west Thailand. At the west coast of Phuket, the maximum water level is 6.5 m and the water level continues to oscillate for long time (Fig. 8a). At the south coast of Phuket the time series begins with a depression of – 3.7 m and the maximum water level reaches up to 4.1 m and the oscillation continues with low amplitudes (Fig. 8b). Fig. 9 shows the similar results at two locations at the north and north-east coasts of Penang Island in Malaysia. At Batu Ferringi (north coast) the maximum elevation is approximately 3.2 m (Fig. 9a). At the location Tanjung Tokong (north-east coast) the maximum elevation is approximately 3.2 m (Fig. 9b). Simulations are also taken out (not shown in the figure) for the other coast locations of Phuket and Penang. The computed results show that, the west coast of Phuket and the north and north-west coasts of Penang Island are vulnerable for stronger tsunami surges.
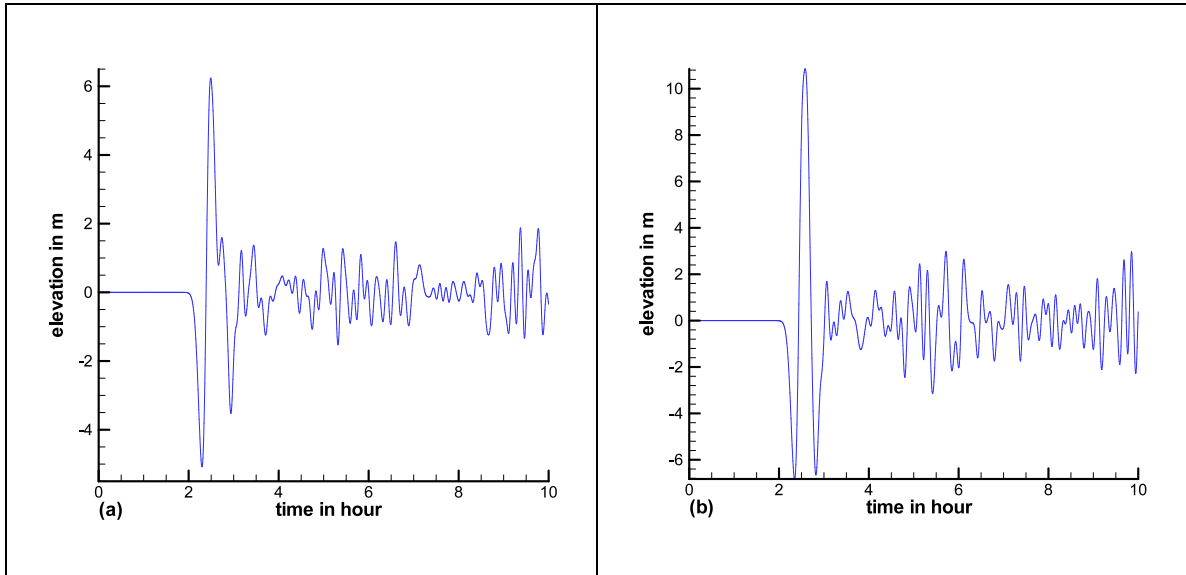
Figure 8: Time series of computed elevation at coastal locations of Phuket: (a) West Phuket,(b) South Phuket.
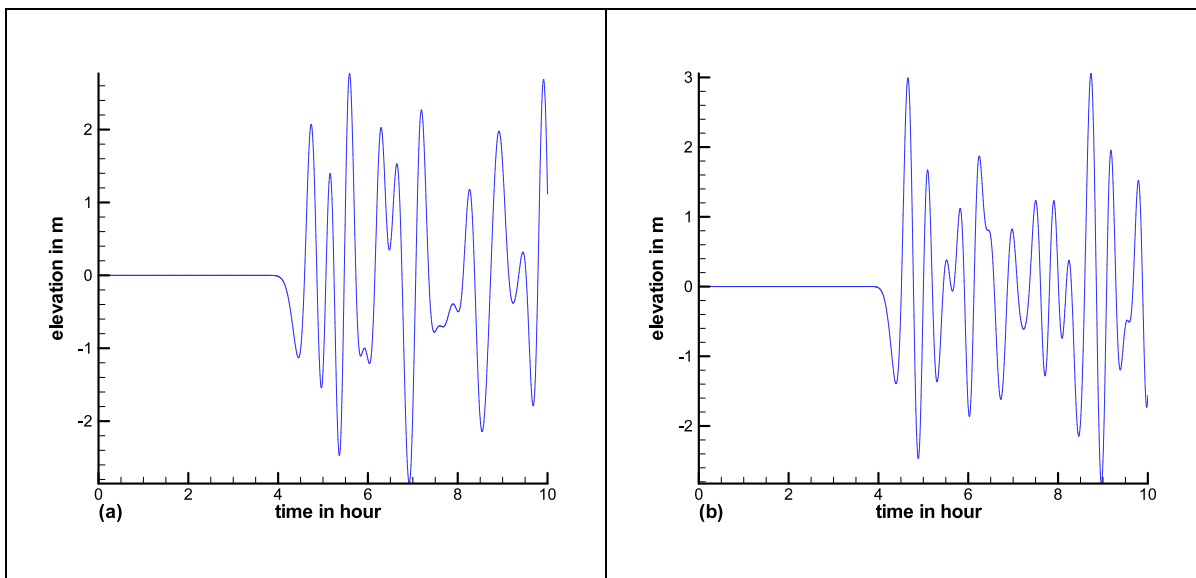

Figure 9: Time series of computed elevation at coastal locations of Penang Island: (a) Batu Ferringhi (b) Tanjung Tokong.

10. CONCLUSIONS

The effect of far field tsunami along the coastal belt of the west coast of Peninsular Malaysia and southern Thailand has been described. A detailed description of the generation of boundary fitted curvilinear grids and the formulation of the boundary condition on this boundary fitted curvilinear grid system is carried out. The tsunami source was removed during the simulation of the far field tsunami along the coastal belts through the open boundary condition. Comparisons between the recorded and simulated waves have been made at two coastal locations of Phuket of Thailand and Penang of Malaysia and good agreement has been found in water elevation. There is a time leg in tsunami propagation time due to the tsunami source and the boundary condition. This time difference can be estimated by measuring the total distance of the open boundary from the coast and tsunami propagation time. So the authors do believe that this approach of simulating far field tsunami can be applied in a limited area model domain where the coastal belts are curvilinear and the bending is high.

REFERENCES

Agarwal, V. K., Agarwal, N. & Kumar, R. (2005). Simulations of the 26 December 2004 Indian Ocean tsunami using a multi-purpose Ocean disaster simulation and prediction model. *Current Science, 88*(3), 439 - 444.

Aida, I. (1974). Numerical Computation of a Tsunami Based on a Fault Origin Model of an Earthquake. *J. Seismol. Soc. Japan, 27*, 141-154.

Aizinger, V., & Dawson, C. (2002). A discontinuous Galerkin method for two-dimensional flow and transport in shallow water. *Advances in Water Resources, 25*(1), 67-84.

Arakawa, A., & Lamb, V. (1977). Computational design of the basic dynamical processes of the UCLA general circulation model. In J. Chang (Ed.), *Methods in Computational Physics* (Vol. 7, pp. 173-265). New York: Academic Press.

Arcas, D., & Titov, V. (2006). Sumatra tsunami: lessons from modeling. *Surv Geophys, 27*, 679 - 705.

Arreaga-Vargas, P., Ortiz, M. & Farreras, S.F. (2005). Mapping the Possible Tsunami Hazard as the First Step Towards a Tsunami Resistant Community in Esmeraldas, Ecuador. In K. Satake (Ed.), *Tsunamis: Case Studies and Recent Developments* (pp. 203 - 215). Netherlands: Springer.

Bao, X.W., Yan, J. & Sun, W. X. (2000). A Three-dimensional Tidal Model in Boundary-fitted Curvilinear Grids. *Estuarine, Coastal and Shelf Science, 50*, 775–788.

Berkman, S. C., & Symons, J.M. (1964). *The tsunami of May 22, 1960 as recorded at tide gauge stations*. Washington, D.C.: U.S. Department of Commerce, Coast and Geodetic Survey.

Cho, Y.-S., Sohn, D.H. & Lee, S.O., (2007). Practical modified scheme of linear shallow-water equations for distant propagation of tsunamis. *Ocean Engineering*, 34, 1769 – 1777.

Haltiner, G. J., & Williams, R.T. (1980). *Numerical Prediction and Dynamic Meteorology*. New York: Wiley.

Heaps, N. S. (1973). A three dimensional numerical model of the Irish Sea. *Geophysics. J. Astron. Soc., 35*, 99 - 120.

Indian Ocean Tsunami at Syowa Station Antarctica. (2007). Retrieved 10 April, 2007, from http://www1.kaiho.mlit.go.jp/KANKYO/KAIYO/KOUHOU/iotunami/iotunami_eng.html

Johns, B., Dube, S.K., Mohanti, U.C., & Sinha, P.C. (1981). Numerical Simulation of surge generated by the 1977 Andhra cyclone. *Quart. J. Roy. Soc. London 107*, 919 – 934.

Johns, B., Rao, A.D., Dube, S.K. & Sinha, P.C. (1985). Numerical modelling of tide–surge interaction in the Bay of Bengal. *Philos. Trans. R. Soc. London Ser. A, 313*, 507–535.

Joolen, V., Givoli, D., & Neta, B. (2003). High-order Non-reflecting Boundary conditions for Dispersive Waves in Cartesian, Cylindrical and Spherical Coordinate Systems. *International Journal of Computational Fluid Dynamics, 17*(4), 263 - 274.

Karim, M. F., Roy, G.D., Ismail, A. I. M. & Meah, M.A. (2006). A Linear Cartesian Coordinate Shallow Water Model for Tsunami Computation along the West coast of Thailand and Malaysia. *International Journal of Ecology &Development, 4*(S06), 1 - 14.

Karim, M. F., Roy, G.D., Ismail, A. I. M. & Meah, M.A. (2007). A Shallow Water Model for Computing Tsunami along the West Coast of Peninsular Malaysia and Thailand Using Boundary- Fitted Curvilinear Grids**,** *Science of Tsunami Hazards*, 26 (1), 21 – 41.

Kowalik, Z., Knight, W., & Whitmore, P. M. (2005). Numerical Modeling of the Tsunami: Indonesian Tsunami of 26 December 2004. *Sc. Tsunami Hazards, 23*(1), 40 – 56.

Murty, T. S. (1977). *Seismic Sea Waves – Tsunamis*. Ottawa: Bull. Fish. Res. Board Canada.

Okada, Y. (1985). Surface Deformation due to Shear and Tensile Faults in a Half Space. *Bull, Seism. Soc. Am., 75*, 1135 - 1154.

Rabinovich, A. B., Thomson, R.E. & Stephenson, F.E. (2006). The Sumatra tsunami of 26 December 2004 as observed in the North Pacific and North Atlantic oceans. *Surveys in Geophysics, 27*, 647 – 677.

Roed, L. P., & Cooper, C.K. (1986). Open boundary conditions in numerical ocean models. In J. J. O'Brien (Ed.), *Advanced Physical Oceanographic Numerical Modeling*: D. Reidel Publishing.

Roy, G. D. (1995). Estimation of maximum water level along the Meghna estuary using a tide and surge interaction model. *Environment International, 21*(5), 671 - 677.

Roy, G. D. (1998). *Mathematical Modeling of Tide, Surge and their Interaction along the Coast of Bangladesh.* Paper presented at the Mini-Workshop on Appl. Math., SUST, Sylhet, Bangladesh.

Roy, G. D. (1999). Inclusion of Off-shore Islands in a Transformed coordinates Shallow Water Model along the Coast of Bangladesh *Environment International, 25*(1), 67 - 74.

Roy, G. D., & Ismail, A. I. M. (2005). *An investigation of 26 December 2004 tsunami waves towards the west coast of Malaysia and Thailand using a Cartesian coordinates shallow water model.* Paper presented at the Int. Conf. Math. & Applications, Mahidol University, Thailand.

Roy, G. D., Karim, M. F., & Ismail, A. M. (2006). Numerical Computation of Some Aspects of 26 December 2004 Tsunami along the West Coast of Thailand and Peninsular Malaysia Using a Cartesian Coordinate Shallow Water Model. *Far East J. Appl. Math., 25*(1), 57-71.

Tang, Y., & Grimshaw, R. (1996). Radiation Boundary Conditions in Barotropic Coastal Ocean Numerical Models. *Journal of Computational Physics, 123*, 96 - 110.

Tsuji, Y., Namegaya, Y., Matsumoto, H., Iwasaki, S.-I., Kanbua, W., Sriwichai, M. & Meesuk, V. (2006). The 2004 Indian tsunami in Thailand: Surveyed runup heights and tide gauge records. *Earth Planets Space, 58*(2), 223-232.

Yoon, S. B. (2002). Propagation of distant tsunamis over slowly varying topography, *Journal of Geophysical Research*, 107, 1 – 11.

Zahibo, N., Pelinovsky, E., Talipova. T., Kozelkov, A. & Kurkin, A. (2006). Analytical and numerical study of nonlinear effects at tsunami modeling. *Applied Mathematics and Computation, 174*(2), 795 - 809.